


RESEARCH ARTICLE

Damage imaging in composites using nonlinear vibro-acoustic wave modulations

L. Pieczonka¹  | L. Zietek¹ | A. Klepka¹ | W.J. Staszewski¹ | F. Aymerich² | T. Uhl¹

¹Department of Robotics and Mechatronics, AGH University of Science and Technology, Krakow, Poland

²Department of Mechanical, Chemical and Materials Engineering, University of Cagliari, Cagliari, Italy

Correspondence

Lukasz Pieczonka, Department of Robotics and Mechatronics, AGH University of Science and Technology, Al. Mickiewicza 30, 30-059 Krakow, Poland.
Email: lukasz.pieczonka@agh.edu.pl

Funding information

Foundation for Polish Science (FNP), Grant/Award Number: WELCOME Programme no. 2010-3/2

Abstract

The paper deals with the application of nonlinear vibro-acoustic modulation technique for detection and localization of impact damage in a laminated composite plate. An imaging procedure—based on the nonlinear vibro-acoustic modulation sidebands—is proposed. The procedure relies on simultaneous low-frequency modal and high-frequency ultrasonic excitations. Laser scanning vibrometry is used to analyze the amplitude of modulation sidebands in vibro-acoustic responses. This analysis is performed for different positions on monitored structure to reveal the location and shape of damage. The method is illustrated using a simple example of impact damage detection in a composite plate. The experimental damage detection results are compared with the results obtained from the previously used approach on the basis of higher harmonic generation. The proposed method demonstrates better ability to locate damage in these comparative tests without the need to increase the measurement bandwidth to the higher harmonics regime. The work shows that the local defect resonance analysis can improve damage detection results of both compared approaches.

KEYWORDS

composites, damage imaging, impact damage detection, local defect resonance, nonlinear acoustics, vibro-acoustic wave modulations

1 | INTRODUCTION

Structural damage detection methods have been constantly evolving to meet requirements of modern engineering applications.^[1,2] The use of advanced materials and manufacturing processes raises the complexity of inspection and requires an ever increasing accuracy of detection. Monitoring and inspection of composite materials is a good example. Nowadays, composites are being adopted for critical structural components. However, it is well known that these materials are often prone to manufacturing defects and in-service damages that are difficult to detect.^[3] Therefore a wide variety of damage detection techniques for assessing structural integrity of composites are used in practice. This includes ultrasound testing, active thermography, radiography, and shearography among others.^[1–3] However, many nondestructive testing (NDT) techniques are labor-intensive, time-consuming, and often expensive to implement for engineering applications. Moreover, NDT inspections are done only at predefined time intervals. Such approach is often not sufficient when dynamic growth of damage needs to be analyzed in monitored structures. Therefore, structural health monitoring (SHM) framework has been introduced in the early 1990s to address this problem.^[4–6] The SHM approach to damage detection is more comprehensive with respect to structural integrity and implementation costs. SHM methods are based on sensors that are integrated with structures and can be used continuously to assess structural health. There are four basic damage identification levels in

SHM, namely,^[4] (a) damage detection, (b) damage localization, (c) damage assessment, and (d) damage prognosis. Damage detection is the first level where only information about the presence of damage is available. The second level augments that information with localization of damage. The third level provides additionally information about the extent/severity and possibly also about the type of damage. Finally, the fourth level assesses structural usage and predicts remaining structural life. Often, the capability of self-diagnosis and self-healing is also considered as an additional fifth SHM level of damage identification.

Various SHM techniques have been developed and are used in practice for structural damage detection, as discussed, for example, in the previous literature.^[2,5–8] Recent years have shown, an increasing interest in novel, the so-called non-classical nonlinear damage detection methods.^[2,9] This is mainly because the nonlinear damage detection methods are usually much more sensitive to detect small damage severities than are their linear counterparts.^[10–12] One of the most promising techniques that can be used for damage detection is a method that utilizes nonlinear vibro-acoustic wave modulations.^[13–15] The method has been successfully applied to detect damage in metallic structures^[16–19] as well as for impact damage detection in composites.^[20–28] The major drawback of this technique is that it offers only the first level damage identification capability, that is, damage detection. Damage localization is not possible when this approach are used in practice.

This paper proposes a nonlinear procedure for damage imaging. The method is based on the non-classical nonlinear effect that involves generation of nonlinear vibro-acoustic modulation sidebands resulting from the interaction of high-frequency (HF) ultrasonic and low-frequency (LF) vibration excitations in the presence of damage. The objective is to localize impact damage in composite materials.

The paper starts with Section 2 that briefly describes the background of nonlinear acoustics and introduces the proposed damage imaging method. Section 3 gives details related to the analyzed composite test sample and to the initial experimental tests performed. The latter includes the impact test—that was performed to generate damage—and the vibrothermographic NDT test that was performed to characterize damage and its location. Section 4 describes the experimental nonlinear acoustic tests undertaken to detect and localize damage. The experimental results from these tests are presented in Section 5, where the proposed method is compared with the higher harmonics imaging technique and its enhancement with the local defect resonance. Finally, the paper is concluded in Section 6.

2 | NONLINEAR ACOUSTICS FOR DAMAGE DETECTION AND LOCALIZATION

This section introduces the method used for damage detection and localization in the current investigations. After a short introduction to nonlinear acoustics, the nonlinear vibro-acoustic technique is briefly described, the existing nonlinear damage localization techniques are reviewed, and the proposed damage localization procedure is presented.

2.1 | Theoretical background

Nonlinear acoustics in the classical form deals with homogeneous materials, where nonlinearity of propagating waves—observed at macroscopic scale—arises from inhomogeneity and physical interactions at microscale and mesoscale.^[9,29] However at the microscale and macroscale, the presence of material discontinuities—such as microcracks or delaminations—leads to the so-called ‘non-classical’ nonlinear phenomena observed in response spectra. The term ‘non-classical’ is used to distinguish the new techniques used for material damage characterization from the classical approach mentioned above. Among many identified manifestations of the ‘non-classical’ behavior are the higher harmonics whose amplitudes do not decay as fast as in the classical case, generation of sub-harmonics, frequency mixing, hysteresis, instabilities, or chaotic dynamics.^[29,30] In the case of planar defects—like the barely visible impact damage (BVID) considered in this study—the contact acoustic nonlinearity^[31] is one of the main nonlinear mechanisms. The contact acoustic nonlinearity results in generation of higher harmonics of unusually high orders with a specific *sinc* modulation of their spectral amplitudes. What is important to note, is that higher harmonics are generated mainly in the area of defect and this phenomenon can be used for damage localization.^[32] There are also other nonlinear mechanisms involved that have been described in the literature: the nonequilibrium dynamics due to the presence of soft inclusions in hard matrix of a material,^[30] hysteretic behavior of certain materials including rocks and some metals,^[30] the Luxembourg–Gorky effect leading to modulation transfer,^[33] dissipative mechanisms,^[16,19,34] or the memory effect.^[34,35] All described mechanisms result in considerable response signal nonlinearities that can be observed and used for damage detection.

2.2 | Vibro-acoustic modulation technique

The nonlinear vibro-acoustic modulation technique relies on an intensive LF (modal) excitation and a weaker HF ultrasonic wave that are introduced to the structure simultaneously,^[15] as illustrated in Figure 1a. The assumption is that, when the monitored material sample is undamaged, response signal spectra exhibit only the major frequency components, that is, the propagating acoustical wave and LF excitation (Figure 1b). However, when the sample is damaged, the spectrum of the response signal reveals additional frequency components such as higher harmonics and modulation sidebands around the HF component (Figure 1c). As mentioned in Section 1, the method—originally developed for fatigue crack detection—has been also successfully applied to impact damage detection in composites.

Previous research investigations—mentioned above—demonstrate that the method is quite sensitive to small damage severities. The analysis of modulation intensity can be also used to assess damage severity. The intensity of modulation is typically described by the parameter R , which is calculated as the ratio between the sum of amplitudes A_{LSB}^i and A_{RSB}^i of the i th pair of left and right modulation sidebands (LSB and RSB, respectively) and the A_{HF} amplitude of the HF component as

$$R = \frac{\sum_{i=1}^n (A_{\text{LSB}}^i + A_{\text{RSB}}^i)}{A_{\text{HF}}} \quad (1)$$

This parameter is often used to discern damaged and undamaged samples and to assess damage severity. The major drawback of this nonlinear vibro-acoustic modulation technique is that the method offers only the first level damage identification capability, that is, damage detection. Damage localization is not possible when this approach is used in practice.

2.3 | State-of-the-art in nonlinear acoustic damage imaging

Several approaches have been proposed in the literature for damage imaging (or damage localization) on the basis of nonlinear system responses.^[36] The common denominator for all these techniques is the possibility of selective imaging of features exhibited by various nonlinear damage-related phenomena. Modulations of single and multiple ultrasonic pulses by LF vibration have been investigated in Didenkulov et al.^[37] As a result, nonlinear scatters from cracks in aluminum and steel rods have been identified experimentally. A similar approach, based on an LF vibration excitation used to perturb damage and HF interrogating wave, was used to detect and localize fatigue crack in aluminum beam in Dziedzic et al.^[38] The authors in Kazakov et al.^[39] analyzed nonlinear wave scatters in solids using the analysis of nonlinear modulations of HF tone bursts by a continuous LF

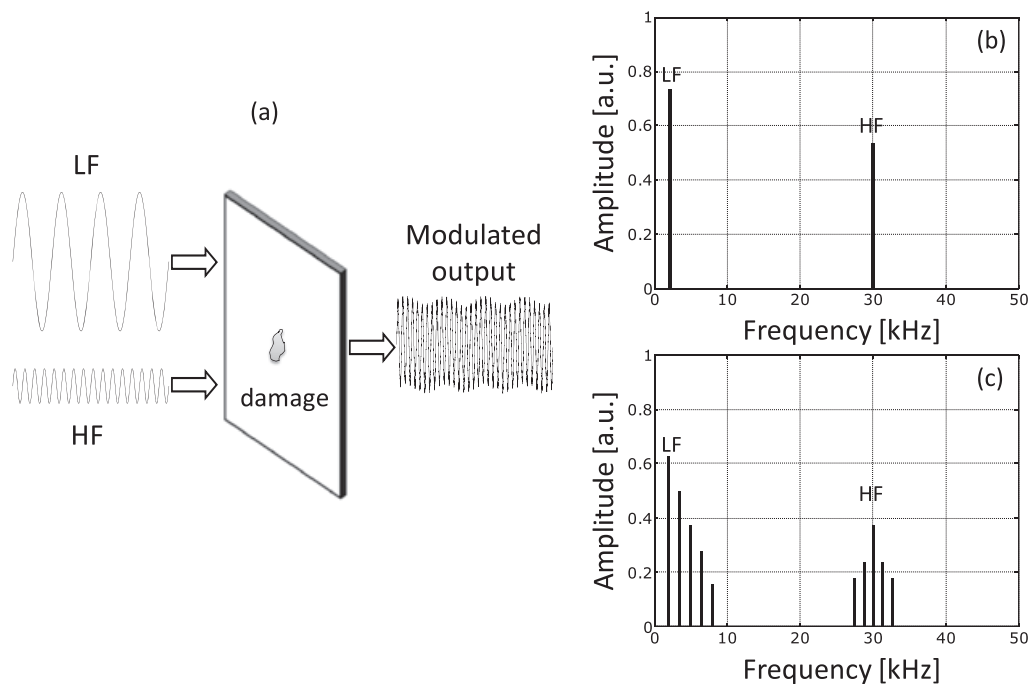


FIGURE 1 The principle of the nonlinear vibro-acoustic modulation technique: (a) schematic diagram illustrating the method; (b) power spectrum of a response signal for an undamaged structure; (c) power spectrum of a response signal for a damaged structure

wave. Experimental verification of the proposed procedure has been demonstrated for a steel plate excited with an electromagnetic shaker and ultrasonic actuator shifted along one of the plate sides. A moving-window and synchronous detection have been used to create spatial mapping revealing nonlinear scatterers in the plate. The subharmonic phased array for crack evaluation has been proposed in Ohara et al.^[40] The technique uses external static or dynamic loads, and short bursts of subharmonic waves have been used to identify nonlinear sources such as closed cracks. A photo-acoustic imaging technique has been proposed in Zakrzewski et al.^[41] The method has relied on the generation of acoustic waves for two different fundamental frequencies. Test sample has been excited with vibration signals generated using a fixed piezoelectric transducer and a moving intensity-modulated laser source. Signals for mixed frequency components—resulting from crack-related nonlinearities—have been captured by a moving accelerometer.

Different approach—based on spatial mapping—has been also proposed in the literature.^[21,32,36,42,43] This approach maps higher harmonics and subharmonics that arise from the presence of damage. The spatial mapping results demonstrate that spectral components related to nonlinear phenomena are strong particularly in the vicinity of damage and therefore can be used for damage localization. The method has been applied successfully to localize damage in metals and composites. The method can be implemented using either the direct spatial distribution of higher harmonic components or the ratio between the amplitude of the second (or third) harmonic over the amplitude of the fundamental harmonic. The latter approach proposed in the literature^[21,42] has been named as the second harmonic imaging technique. Higher harmonic components were also considered in the context of structural integrity maps used for damage localization.^[44,45] More recently, an enhancement of the higher harmonics mapping technique—based on the concept of the local defect resonance (LDR)^[46,47]—has been proposed. The foundation of the LDR method is an observation that structural damages always have a set of associated structural resonances that depend on the type, size, and geometry of damage. Once these resonances are established, the relevant damage-related resonance frequencies (LDR frequencies) can be used for excitation to reveal damage in nonlinear acoustic tests. This is mainly because when a structure is excited with a monoharmonic signal at a frequency corresponding to one of the LDR frequencies, the vibration energy is delivered selectively to the damaged locations. In turn, the amplitude level of higher harmonics in measured response spectra increases dramatically. The amplitude level of higher harmonics in this case is much higher than that in the case of arbitrarily selected excitation frequencies. This is why spatial mapping of measured spectral amplitudes, at frequencies equal to higher harmonics of LDR frequencies, can lead to damage localization.

Previous research investigations show that LDR frequencies can be estimated using a laborious experimental approach or numerical simulations. This is not an easy task because the former requires excitation with broadband sweeping frequencies, whereas the latter needs good models of damage. In addition, some a priori knowledge of damage is needed in practice to obtain good damage detection results.

It is important to note that imaging capability of nonlinear acoustic techniques is not only important in engineering applications for damage localization. It is well known that many nonlinear effects—such as higher harmonic generation or vibro-acoustic modulations—are produced not only by damage but also by intrinsic effects, for example, material nonlinearities, boundary conditions, or measurement chain. It is clear that a reliable procedure for damage imaging in nonlinear acoustics could identify where the main sources of nonlinearity are to distinguish damage-related from intrinsic effects.

2.4 | Damage imaging approach based on modulation sidebands

Nonlinear higher harmonic generation is highly localized and particularly strong in the vicinity of damage, as described in Section 2.3. The assumption is that nonlinear modulation sidebands will exhibit the same localized property, without the need to increase the measurement bandwidth to the higher harmonics regime. Therefore, sideband imaging—rather than higher harmonic imaging—is proposed for damage localization. The procedure proposed for damage localization is exactly the same as the procedure used for damage detection shown in Figure 1, that is, surface-bonded piezoceramic transducers are used for excitation and a laser vibrometer is used for response measurement. However, in contrast to the typical damage detection test, responses are acquired for a predefined grid on the entire surface of monitored specimens using the scanning capability of laser vibrometer. Power spectra from measured responses are calculated to reveal modulation sidebands at frequencies equal to $HF \pm n \cdot LF$, where n is a positive integer. The modulation intensity—based on the amplitude of sidebands—is then analyzed for all scanned points to reveal areas of large modulation intensities due to structural damage. In the proposed case, the modulation intensity defined by the mean value of the first modulation sidebands amplitudes is mapped.

In principle, the proposed technique is similar to the previously used spatial mapping-based methods reviewed in Section 2.3. However, in contrast to higher harmonics and subharmonics-based methods, the nonlinear modulation sidebands are used for damage localization. Also, in contrast to^[42] noncontact scanning acquisition—provided by a laser vibrometer—is used

instead of noncontact scanning photo-acoustic laser excitation. It is well known that a photo-acoustic laser used for excitation can damage the surface of monitored structures due to extensive heating and ablation.

3 | DAMAGED COMPOSITE PLATE

This section presents a composite specimen used in nonlinear acoustic imaging tests. Hidden impact damage—introduced by an impact—is identified and described using a classical vibrothermographic NDT procedure.

3.1 | Composite plate

The test sample investigated was a laminated composite plate with a BVID. The plate was manufactured from carbon/epoxy (Seal HS160/REM) unidirectional prepreg plies. The stacking sequence of the laminate was $[0_3/90_3]_s$. The dimensions of the plate were $150 \times 300 \times 2$ mm. The specimen was nondestructively verified—using X-ray—to be free from manufacturing defects prior to testing. The dimensions and details of the plate are shown in Figure 2.

3.2 | Impact testing

Low velocity impact test was performed on the plate to introduce damage. The plate was simply supported on a rigid post with a rectangular opening in the center, and an instrumented drop-weight testing machine was employed to impact the plate in the central location. The plate was impacted with the energy of 3.9 J, which was obtained by selecting the appropriate drop height of the impactor. The absorbed energy was evaluated by measuring (by an infrared sensor) the velocities of the impactor immediately before and after the impact; the contact force was measured by means of a semiconductor strain-gage bridge bonded to the indenter. The force-time curve and the force-displacement curve acquired during the impact test are presented in Figure 3.

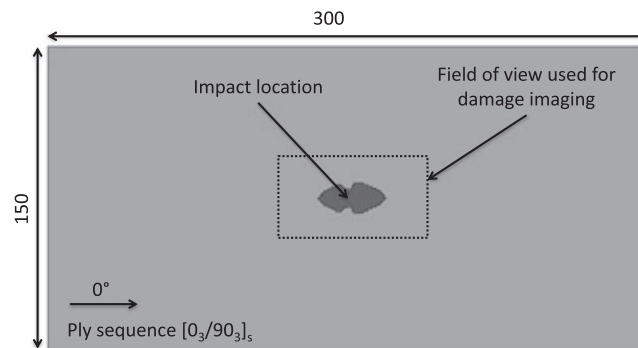


FIGURE 2 Carbon/epoxy prepreg plate with the barely visible impact damage (dark area in the center of the plate) used in nonlinear damage detection tests

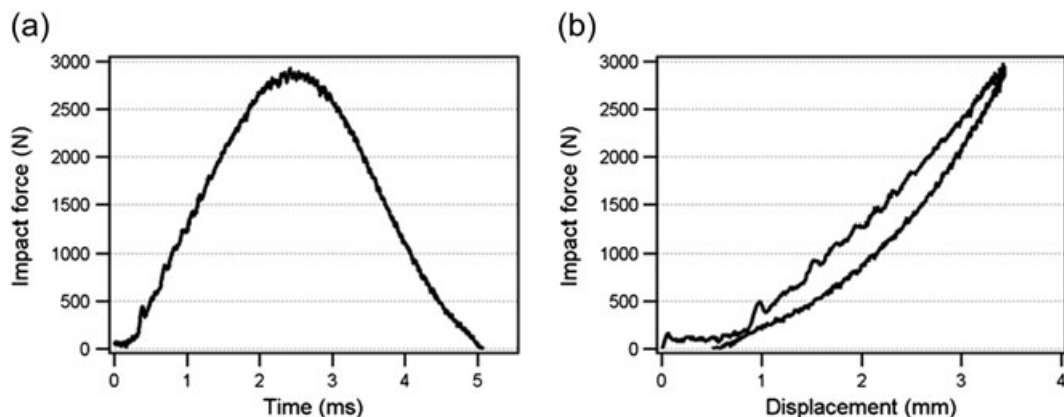


FIGURE 3 Impact characteristics: (a) force-time curve and (b) force-displacement curve

3.3 | Damage characterization with vibrothermography

After conducting impact test, the extent of damage in the plate was evaluated using vibrothermography. The method used is an active thermographic NDT technique with external excitation.^[48,49] In vibrothermography, external energy is delivered to monitored structure by ultrasonic vibrations. Typically, a burst signal with the duration of several milliseconds is used to excite a test sample. HF vibrations cause energy dissipation at material discontinuities (i.e., cracks and delaminations), and mechanical energy is converted into heat. Thermographic camera was used to record the surface temperature distribution on the tested sample. Inference about the existence of damage is performed on the basis of the measured temperature distribution. Vibrothermography is a dark field method where the source of heat is the damage itself, which simplifies the data processing phase to a great extent.

The *Monit SHM* mobile vibrothermographic test system—with the 35 kHz ultrasonic excitation column—was used to conduct the experiment.^[50] The photon detector camera *Cedip Silver 420 M* was applied to acquire thermal image sequences. The ultrasonic column was exciting the plate for 500 ms, and thermographic camera was acquiring the signal at 100 Hz frame rate for 3 s.

The results from the vibrothermographic inspection are shown in Figure 4. This figure presents temperature distribution measured on the surface of the plate in the central area marked by the dashed line in Figure 2. Background temperature distribution, measured just before the beginning of the test, was subtracted from the results to improve the contrast. There are four different time instances shown in Figure 4. Time $t = 0$ ms corresponds to the start of the ultrasonic excitation of the sample. Here, the temperature distribution is uniform and only the thermal camera detector noise is present. After $t = 100$ ms, the vertical surface matrix cracks are becoming visible in the thermal picture. After $t = 200$ ms, a characteristic butterfly like delamination on the $0^\circ/90^\circ$ interface further from the impact side is revealed. Finally, after $t = 400$ ms, the picture starts to become blurred. This is mainly due to the temperature being conducted away from the source, which in the case of vibrothermography is the damage itself. The area of delamination after the 3.9 J impact was identified from the test as approximately 300 mm^2 . In summary, the NDT test performed revealed the shape and size of damage.

4 | NONLINEAR ACOUSTIC DAMAGE IMAGING

Once the delamination was identified in the composite plate, a series of experimental nonlinear imaging tests were performed. Experimental testing for nonlinear damage imaging was performed using two different measurement approaches based on (a) the higher harmonics and (b) the proposed vibro-acoustic modulation sidebands. Both approaches were used with a set of excitation frequencies, including the LDR frequency of the BVID. The experimental set-up—illustrated in Figure 5—was used in all tests. The composite plate was suspended using elastic cords to simulate free-free boundary conditions and to avoid nonlinear boundaries. The LF excitation was applied to the plate using a surface-bonded *Noliac CMAP4* stack actuator. At the same time, the HF excitation was also applied to the plate using a low-profile, surface-bonded *PI Ceramic* 15×1 mm piezoelectric disc. Both transducers were driven by the *Agilent 33522A* signal generator and *EC Systems PAQG* signal amplifier. The latter was used to magnify the amplitude of excitation. A *Polytec PSV-400* scanning laser vibrometer was used for noncontact measurements of vibration responses.

Selection of the LF and HF excitation frequencies is the first important step in the nonlinear acoustic tests. This selection is particularly important for the local frequency of damage. Experimental modal analysis can be used in practice to reveal the LDR. However, it is important to note that this experimental investigation is time-consuming due to the analysis of mode shapes

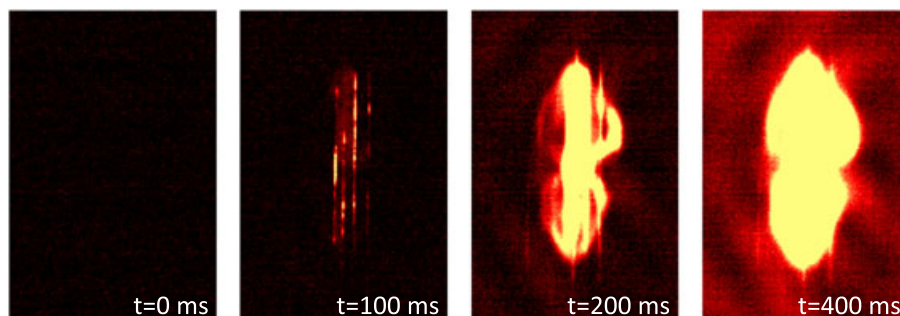


FIGURE 4 Results of the vibrothermographic measurement on the composite plate—Surface temperature distribution at different time instances

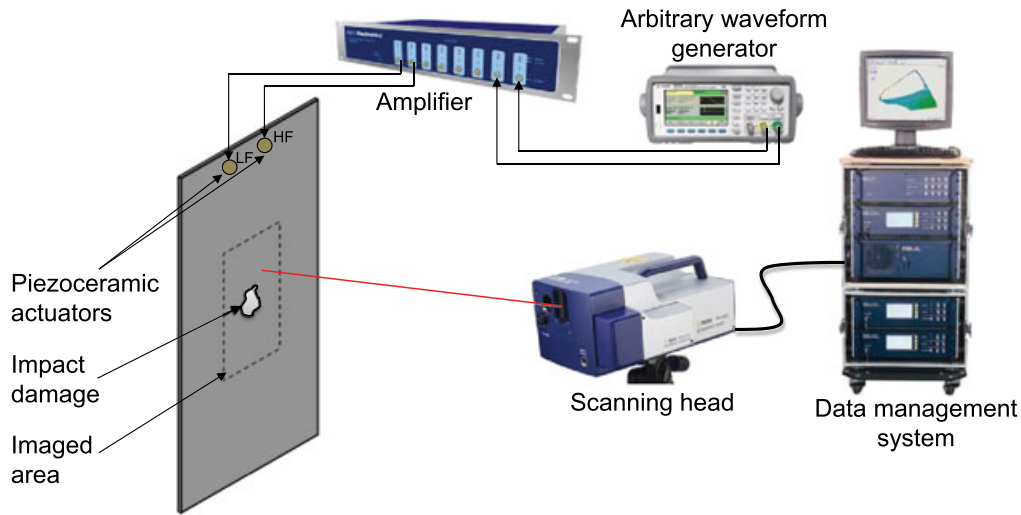


FIGURE 5 Experimental set-up used for the nonlinear acoustic imaging

for a broad range of sweeping excitation frequencies. This test is not easy when small damage is involved because vibration measurements need to be taken on a dense network of measurement points in order not to miss the location of defect. In addition, the LDR frequency is typically in the HF range where modal density (the number of natural frequencies per Hz) is very high. Because, in the analyzed case, the extent and location of damage was known from the NDT tests, the LDR value could be calculated prior to experimental testing. Due to the complex shape of the delamination revealed in Section 3.3 and the anisotropy of the composite material calculation of the LDR frequency using an analytical formula was not possible. Instead, a more general approach using finite element (FE) modeling was used to predict the LDR value, as described in the next section.

4.1 | Numerical modal analysis

A simple FE model of the damaged plate was developed using the *MSC.Patran* pre-processor. The plate was discretized using linear hexahedral solid finite elements with the size of $0.5 \times 1 \times 1$ mm resulting in four elements across the thickness of the plate. One solid element was representing three composite plies with the same orientation in order to reproduce the desired ply stacking sequence. The BVID was modeled by the introduction of double nodes in the FE mesh between the 90° and the 0° plies that were located farthest from the impacted side. As a result, neighboring finite elements were disconnected in the desired area. The model of delamination followed the exact shape of damage revealed by the NDT tests. The values of material parameters used in these simulations are given in Table 1.

Once the model was developed, modal analysis was performed. Natural frequencies and mode shapes were obtained by solving the free undamped vibration problem. The contact interaction and friction at the delaminated interface were therefore not modeled to simplify the problem. The *MSC.Nastran* FE solver was used to perform numerical computations. The normal modes solution (SOL103) was applied to find vibration mode shapes of the delaminated composite plate. Following these investigations, the LDR was identified for the frequency of 29,852 Hz excitation. The corresponding mode shape is presented in Figure 6.

4.2 | Experimental modal analysis

Subsequently, experimental modal analysis was performed to confirm the findings from the numerical model. The experiment was performed using the arrangements shown in Figure 5. The *Noliac CMAP4* piezoelectric stack actuator was driven with a white noise signal. The excitation voltage amplitude was equal to $80 V_{p-p}$. The scanning laser vibrometer was used for non-contact measurements of vibration responses at 435 points on a 15×29 measurement symmetrical rectangular grid. The

TABLE 1 Mechanical properties of the composite material used in the FE model.

$E_x = 93.7$ GPa	$E_y = 7.45$ GPa	$G_{xy} = 3.97$ GPa	$\nu_{xy} = 0.261$	$\rho = 1.5$ g/mm ³
------------------	------------------	---------------------	--------------------	--------------------------------

Note. FE = finite element.

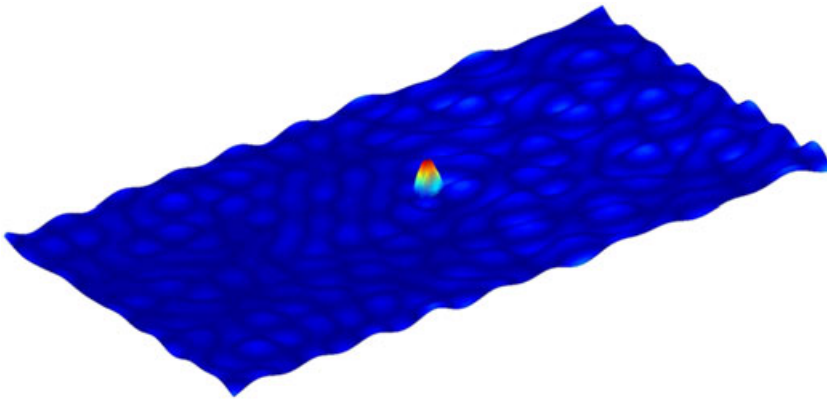


FIGURE 6 Mode shape of the local defect resonance frequency at 29 852 Hz revealed by numerical simulations

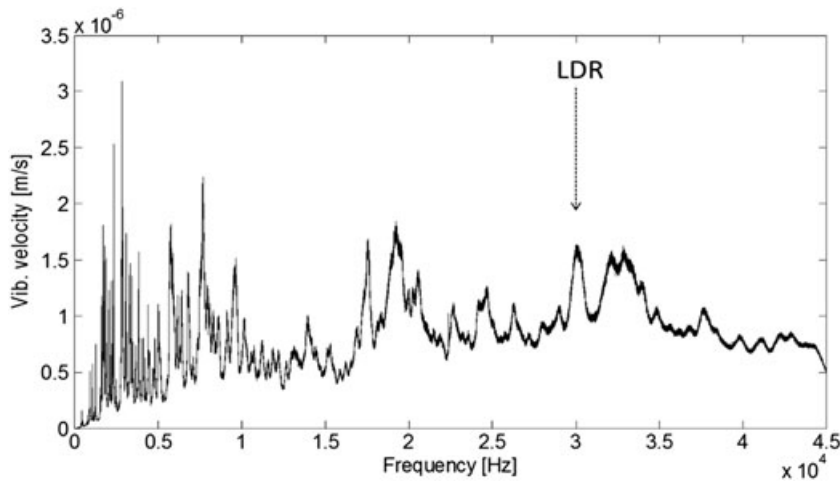


FIGURE 7 Experimental FRF for the analyzed damaged composite plate

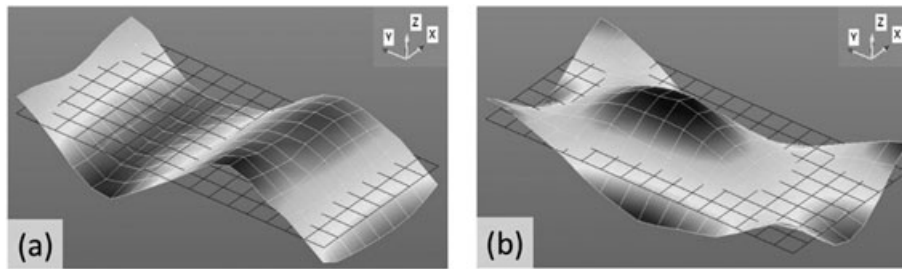


FIGURE 8 Mode shapes corresponding to f_{LF1} (a) and f_{LF2} (b) frequencies selected as low-frequency excitation in vibro-acoustic modulation tests

analysis was performed in the frequency range from 0 to 45 kHz. Figure 7 gives the averaged frequency response function (FRF)—estimated from the responses in the central part of the plate—for the analyzed frequency range. The analysis of modes shapes between 25 and 35 kHz revealed the LDR frequency at 30 095 Hz. This frequency value was very close to the value predicted from the numerical model.

Once the LDR frequency was identified, the LF frequency had to be selected. The frequency of one of the first structural responses is typically chosen for the LF excitation in the nonlinear vibro-acoustic modulation technique used for damage detection. The frequencies of $f_{LF1} = 461$ Hz and $f_{LF2} = 491$ Hz, corresponding to the strong LF resonances, were selected in the current investigations. The delamination, located in the center of the plate, was located around the node of vibrations for the first mode and around the antinode of vibrations for the second mode, as can be seen in Figure 8a,b, respectively. The motivation behind this choice was to verify possible influence of the LF mode shape on the damage imaging quality.

Three different frequencies were selected for the HF excitations in the nonlinear imaging tests, that is, $f_{HF1} = 43\,000$ Hz; $f_{HF2} = 30\,095$ Hz, and $f_{HF3} = 50\,000$ Hz. Two frequencies f_{HF1} and f_{HF3} were selected arbitrarily and f_{HF2} was the identified LDR frequency. The LDR frequency was already used in the nonlinear vibro-acoustic modulation tests in previous research

work presented in Klepka et al.^[27] The results of that work reveal that combining the LF pumping excitation wave with the LDR probing excitation greatly enhances the damage detection capability of the nonlinear vibro-acoustic modulation technique.

5 | EXPERIMENTAL RESULTS FROM DAMAGE DETECTION USING NONLINEAR ACOUSTIC IMAGING

Once the excitation frequencies were selected, the nonlinear damage imaging tests were performed. Laser scanning and damage imaging was performed for the area of the composite plated indicated by the dashed line in Figure 2. This section presents the results from these experimental investigations. First, the results for higher harmonic generation are presented. Then the results for the proposed nonlinear imaging method based on modulation sidebands are given.

5.1 | Higher harmonics imaging

Single-harmonic excitation corresponding to the selected HF frequencies, that is, $f_{HF1} = 43,000$ Hz; $f_{HF2} = 30,095$ Hz, and $f_{HF3} = 50,000$ Hz were used in the damage detection imaging technique on the basis of higher harmonic generation. The experimental results from these investigations are presented in Figure 9. Spatial mapping of the spectral amplitudes corresponding to the first harmonic components (Figure 9a–c) and the second harmonic components (Figure 9d–f) are presented. The amplitudes are presented in linear scale and have been normalized to allow easier comparison between different frequencies. In case of linear images for f_{HF1} and f_{HF3} presented in Figure 9a,c, no clear indication of the presence or location of damage can be observed.

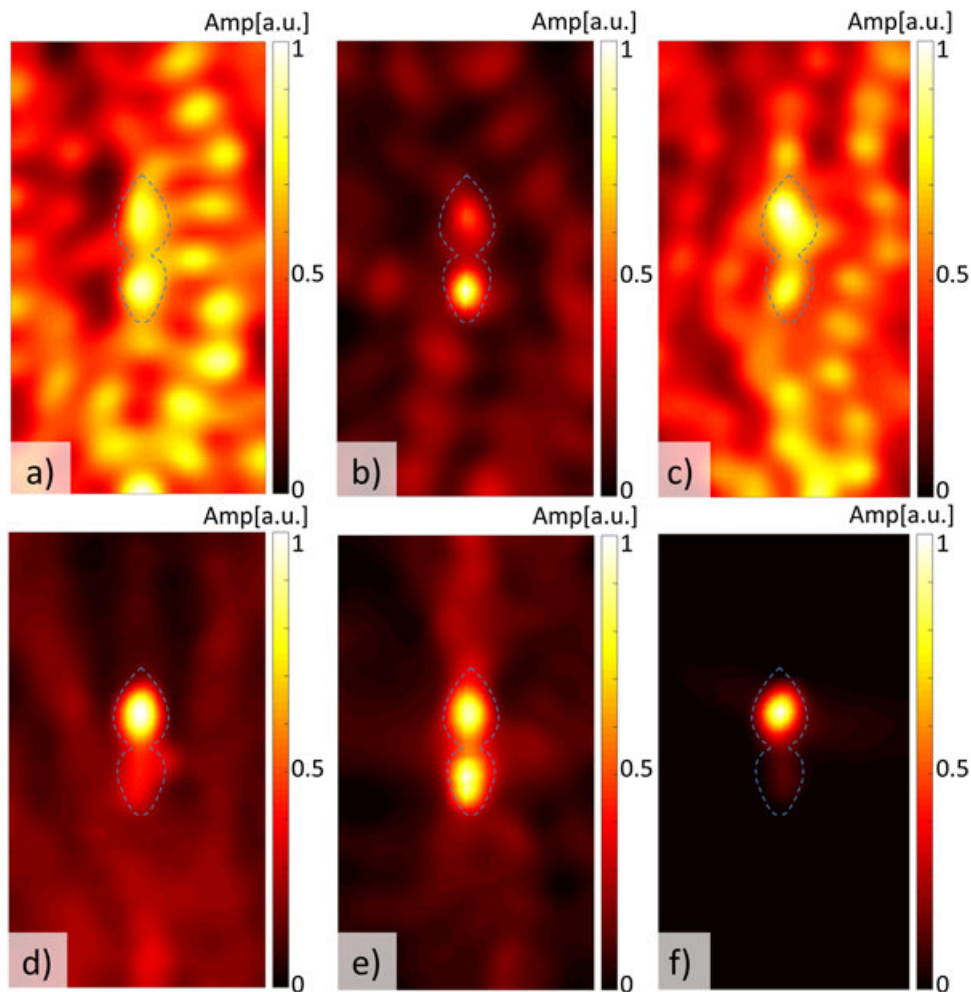


FIGURE 9 Linear (a–c) and nonlinear (d–f) imaging based on higher harmonics generation. Spectral intensity maps for the excitation frequencies equal to: (a) $f_{HF1} = 43$ kHz; (b) $f_{HF2} = 30.095$ kHz; (c) $f_{HF3} = 50$ kHz and for their second harmonics (d) $2f_{HF1} = 86$ kHz; (e) $2f_{HF2} = 60.190$ kHz; (f) $2f_{HF3} = 100$ kHz. Contour of damage is indicated with a dashed line

Spectral amplitude levels on BVID are comparable to the amplitude levels in the surrounding. The linear image for f_{HF2} corresponding to the LDR frequency (Figure 9b) already indicates the presence and the location of the BVID in the central part of the image. In contrast, the nonlinear images for all frequencies, shown in Figures 9d–f, clearly indicate the presence and the location of damage. The results confirm the localization effect of higher harmonics known from the literature. In addition, the results clearly show that the excitation with the LDR frequency enhances damage detection. The location of delamination can be clearly identified in all three cases, but the nonlinear image involving the second harmonic of the LDR frequency in Figure 9e exhibits the shape of the analyzed delamination in a more precise way. It is, however, important to note that the previous research studies—reported in^[51]—demonstrate that other selected excitation frequencies in this test may produce less clear damage images.

5.2 | Vibro-acoustic modulation sideband imaging

Subsequently, the proposed imaging procedure based on the nonlinear vibro-acoustic modulation sidebands was applied to the damaged composite plate. Figure 10 presents the results of the imaging procedure. The modulation intensity defined by the mean value of the first modulation sidebands amplitudes is mapped and analyzed in these figures. Figure 10a–c correspond to the first selected natural frequency of the plate at $f_{LF1} = 461$ Hz (shown in Figure 8a) combined with three HF excitations: $f_{HF1} = 43$ kHz, $f_{HF2} = 30.095$ kHz and $f_{HF3} = 50$ kHz, respectively. Figures 10 d–f correspond to the second selected natural frequency of the plate at $f_{LF2} = 491$ Hz (shown in Figure 8b) and the same set of high frequencies as before. As can be seen, the damage can be easily identified in all considered cases. The amplitude contrast between the damaged area and the surrounding

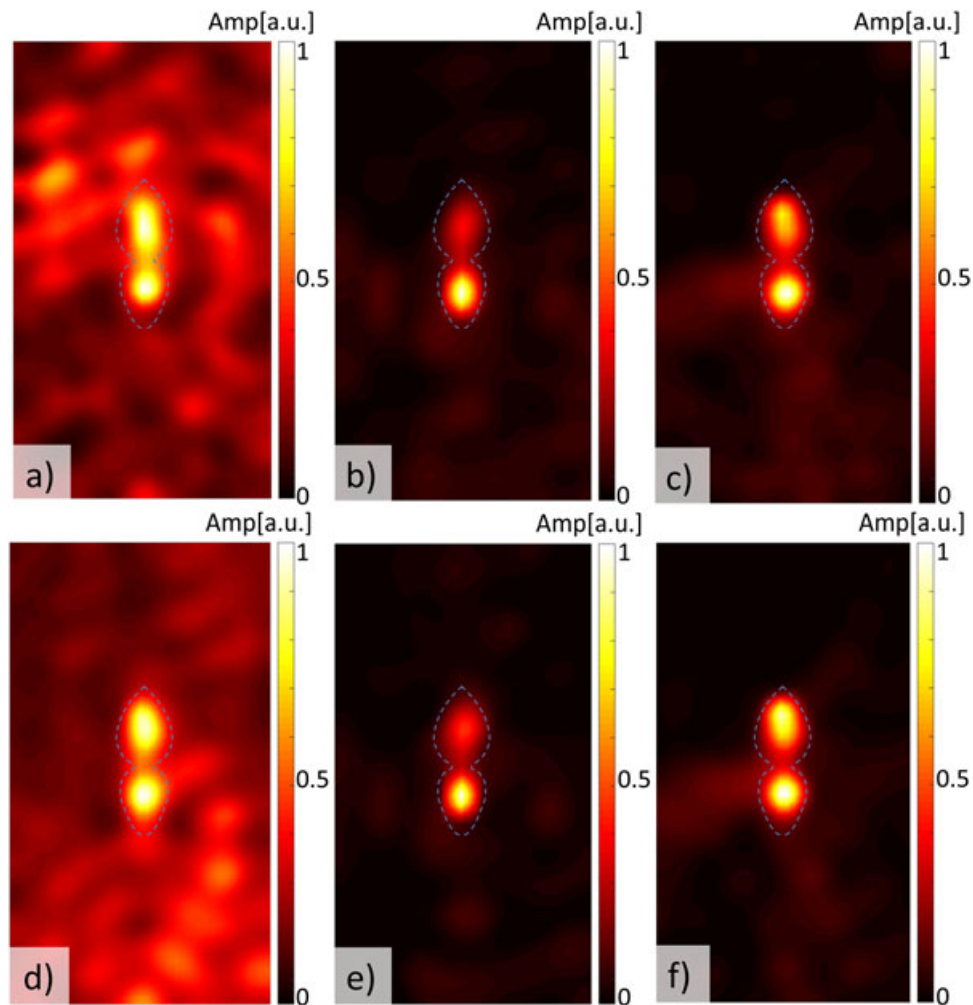


FIGURE 10 Vibro-acoustic modulation sideband imaging results for (a) $f_{LF1} = 461$ Hz and $f_{HF1} = 43$ kHz; (b) $f_{LF1} = 461$ Hz and $f_{HF2} = 30.095$ kHz; (c) $f_{LF1} = 461$ Hz and $f_{HF3} = 50$ kHz; (d) $f_{LF2} = 491$ Hz and $f_{HF1} = 43$ kHz; (e) $f_{LF2} = 491$ Hz and $f_{HF2} = 30.095$ kHz; (f) $f_{LF2} = 491$ Hz and $f_{HF3} = 50$ kHz. Contour of damage is indicated with a dashed line

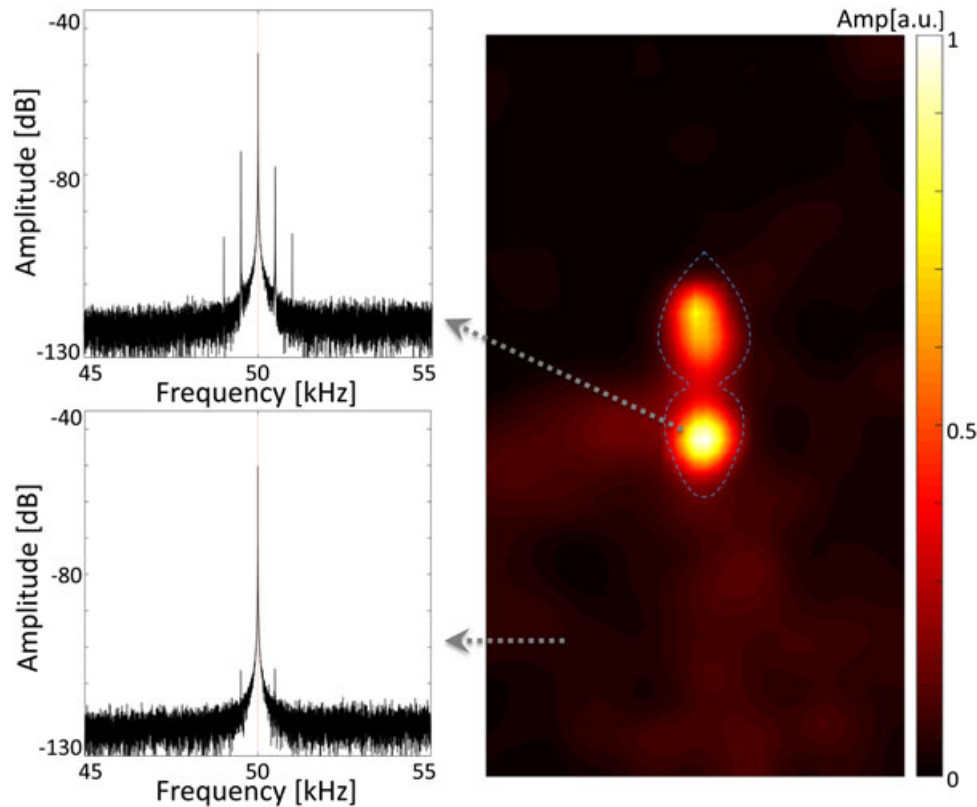


FIGURE 11 Comparison of frequency spectra measured at two different locations on the plate for excitation frequencies equal to $f_{LF2} = 491$ Hz and $f_{HF3} = 50$ kHz

is different for the particular combinations of excitation frequencies. However, the location and shape of the BVID can be clearly seen in the central part of the plate irrespectively of the frequency combinations. The results confirm that the localization effect of the modulation sidebands is strong around the nonlinearity source, similarly to the case of higher harmonics components. Moreover, the selection of excitation frequencies is not critical for the imaging process. In particular, the results obtained for two different modal frequencies f_{LF1} and f_{LF2} are nearly the same, as can be seen in Figure 10. Moreover, the LDR frequency at $f_{HF2} = 30.095$ kHz produced the results (shown in Figure 10b,e) comparable with the results obtained with an arbitrarily selected an arbitrarily selected $f_{HF3} = 50$ kHz (shown in Figure 10c,f). This was not the case for the higher harmonics imaging where the selection of LDR excitation clearly enhanced the imaging quality.

Finally, Figure 11 shows the comparison of frequency spectra measured at two different locations on the plate for excitation frequencies equal to $f_{LF2} = 491$ Hz and $f_{HF3} = 50$ kHz. As can be seen, the level of modulation sidebands is much higher around the BVID location compared with that in the healthy area of the plate. These results show a great potential for the proposed nonlinear damage imaging procedure. However, they also indicate that a proper choice of the measurement point for the classical nonlinear vibro-acoustic modulation testing is very important. Although the modulation sidebands can be seen in all measurement points across the plate, the amplitude level of sideband components is significantly different depending on the location on the plate. The inappropriate choice of a measurement location may lead to an unsuccessful detection in the presence of measurement noise or in a difficulty to select a proper detection threshold.

6 | CONCLUSIONS

Two different experimental nonlinear imaging techniques were performed to reveal the presence and location of delamination the composite plate. The basic approach—previously described in the literature—was based on spatial mapping of higher harmonics arising under single-harmonic excitation. This basic approach exhibited the location of damage correctly but not always mirrored the complex shape of delamination. The imaging technique based on higher harmonic generation was enhanced by the application of LDR frequency for the monoharmonic excitation. This enhancement improves the results, so the revealed location and shape of damage are clearer. However, the major problem with this approach is that the estimation of the LDR

frequency requires some prior knowledge on damage (when numerical simulations are used) and may be time-consuming (when estimated experimentally). In addition, this estimation could be problematic for small damage severities and multiple damages.

An imaging procedure—based on the nonlinear modulation sidebands resulting from vibro-acoustic interactions—has been proposed. The method utilizes the same experimental set-up that is typically used for the nonlinear vibro-acoustic modulation technique and helps to identify the sources of nonlinearity in a structure. The method is relatively simple and—what is important—does not require the knowledge of the LDR frequency to obtain satisfactory results. However, if the LDR frequency is known or can be easily estimated, the application of this frequency for the HF excitation in the proposed imaging technique can further improve damage detection results.

The experimental results show that the proposed nonlinear imaging technique—based on vibro-acoustic modulation sidebands—produces more accurate results if compared with similar techniques based on higher harmonic generation. The improvement is in terms of both damage location and the ability to mirror the shape of damage. Moreover, the tests can be performed without the need to go to the higher harmonics regime, allowing to save measurement bandwidth. A number of different combinations of LF and HF frequencies were analyzed; not all of them were reported in this paper, in order to check the robustness of the proposed damage imaging procedure. A general observation is that the location of damage is always revealed in those images, whereas the shape and the extent of damage are much less certain. As such, we see the proposed damage imaging method as a valuable research tool, which can aid in distinguishing damage-related from intrinsic nonlinear effects by localizing the sources of nonlinearities in a structure.

Further research work is needed to confirm the above findings. Future work should investigate various types of damage and different severities of damage. The problem of damage detection sensitivity for different excitation frequencies should be investigated. There is also some scope for work related to image processing and to damage detection probabilities.

ACKNOWLEDGEMENTS

The research was financed by the Foundation for Polish Science (FNP) within the scope of the WELCOME Programme no. 2010-3/2.

REFERENCES

- [1] P. O. Moore (Ed), *Nondestructive Testing Handbook, Overview*, American Society for Nondestructive Testing **2012**.
- [2] T. Stepinski, T. Uhl, W. J. Staszewski, *Advanced Structural Damage Detection: From Theory to Engineering Applications*, Wiley, Chichester **2013**.
- [3] J. E. Masters, *Damage Detection in Composite Materials. Philadelphia: ASTM STP 1128*, American Society for Testing and Materials **1992**.
- [4] Rytter A. Vibration based inspection of civil engineering structures. Ph.D. Dissertation, Department of Building Technology and Structural Engineering, Aalborg University, Denmark, **1993**.
- [5] W. J. Staszewski, C. Boller, G. R. Tomlinson, *Health Monitoring of Aerospace Structures: Smart Sensor Technologies and Signal Processing*, Wiley, Chichester **2004**.
- [6] D. Balageas, *Structural Health Monitoring*, Wiley-ISTE, London **2006**.
- [7] M. Ohtsu, *Mag. Concr. Res.* **1996**, *48*, 321.
- [8] A. Carpinteri, G. Lacidogna, A. Manuello, G. Niccolini, *Struct. Control Health Monit.* **2016**, *2016(23)*, 659.
- [9] P. P. Delsanto (Ed), *Universality of Nonclassical Nonlinearity: Applications to Non-Destructive Evaluations and Ultrasonics*, New York, Springer **2006**.
- [10] V. Yu. Zaitsev, A. M. Sutin, I. Yu. Belyaeva, V. E. Nazarov, *J. Vib. Control* **1995**, *1(3)*, 335.
- [11] P. B. Nagy, *Ultrasonics* **1998**, *36*, 375.
- [12] I. Y. Belyaeva, V. Y. Zaitsev, *J. Vib. Control* **1996**, *2(4)*, 465.
- [13] D. M. Donskoy, A. M. Sutin, *J. Intel. Mater. Syst. Struct.* **1999**, *9*, 765.
- [14] K. Van Den Abeele, P. A. Johnson, A. M. Sutin, *Res. Nondestruct. Eval.* **2000**, *12*, 17.
- [15] L. Pieczonka, A. Klepka, A. Martowicz, W. J. Staszewski, *Optic. Eng.* **2015**, *55(1)*, 011005.
- [16] V. Zaitsev, P. Sas, *J. Vib. Control* **2000**, *6*, 803.
- [17] Z. Parsons, W. J. Staszewski, *Smart Mat. Struct.* **2006**, *15(4)*, 1110.
- [18] P. Duffour, M. Morbidini, P. Cawley, *J. Acoust. Soc. Am.* **2006**, *119(3)*, 1463.
- [19] A. Klepka, W. J. Staszewski, R. B. Jenal, M. Szwedko, J. Iwaniec, T. Uhl, *Struct. Health Monitor.* **2011**, *11(2)*, 197.

- [20] M. Meo, G. Zumpano, *Composite Struct.* **2005**, *71*, 469.
- [21] U. Polimeno, M. Meo, D. P. Almond, *Adv. Sci. Tech.* **2008**, *56*, 426.
- [22] F. Aymerich, W. J. Staszewski, *Structur. Health Monitor.* **2010**, *9*(6), 541.
- [23] F. Aymerich, W. J. Staszewski, *Compos. A: Appl. Sci. Manuf.* **2010**, *41*(9), 1084.
- [24] L. Pieczonka, W. J. Staszewski, T. Uhl, *Key Eng. Mater.* **2013**, 569–570, 96.
- [25] L. Pieczonka, A. Klepka, W. J. Staszewski, T. Uhl, F. Aymerich, *Key Eng. Mater.* **2013**, 558, 341.
- [26] L. Pieczonka, P. Ukowski, A. Klepka, W. J. Staszewski, T. Uhl, F. Aymerich, *Smart Mater. Struct.* **2014**, *23*(10), 105021.
- [27] A. Klepka, L. Pieczonka, W. J. Staszewski, F. Aymerich, *Compos. Part B Eng.* **2014**, *65*, 99.
- [28] A. Klepka, W. J. Staszewski, D. di Maio, F. Scarpa, *Smart Mat. Struct.* **2013**, *22*(8), 084011.
- [29] M. F. Hamilton, D. T. Blackstock, *Nonlinear Acoustics*, Academic Press, San Diego **1998**.
- [30] R. A. Guyer, P. A. Johnson, *Nonlinear Mesoscopic Elasticity: The Complex Behaviour of Rocks, Soil, Concrete*, Wiley-VCH, Weinheim **2009**.
- [31] I. Y. Solodov, N. Krohn, G. Busse, *Ultrasonics* **2002**, *40*, 621.
- [32] N. Krohn, R. Stoessel, G. Busse, *Ultrasonics* **2002**, *40*, 633.
- [33] V. Zaitsev, V. Gusev, B. Castagnede, *Ultrasonics* **2002**, *40*(1), 627.
- [34] V. Zaitsev, V. Gusev, B. Castagnede, *Phys. Rev. Lett.* **2003**, *90*(7), 075501.
- [35] I. Y. Solodov, B. Korshak, *Phys. Rev. Lett.* **2002**, *88*, 014303.
- [36] W. S. Gan, *Acoustical Imaging: Techniques and Applications for Engineers*, Wiley, Chichester **2012**.
- [37] I. N. Didenkulov, A. Sutin, V. V. Kazakov, A. Ekimov, S. W. Yoon, *AIP Conf. Proc.* **2000**, *524*, 329.
- [38] K. Dziedzic, L. Pieczonka, P. Kijanka, W. J. Staszewski, *Struct. Control Health Monit.* **2016**, <https://doi.org/10.1002/stc.1828>.
- [39] V. Kazakov, A. Sutin, P. A. Johnson, *Appl. Phys. Lett.* **2002**, *81*(4), 646.
- [40] Y. Ohara, T. Mihara, R. Sasaki, T. Ogata, S. Yamamoto, Y. Kishimoto, K. Yamanaka, *Appl. Phys. Lett.* **2007**, *90*(1), 011902.
- [41] J. Zakrzewski, N. Chigarev, V. Tournat, V. Gusev, *Int. J. Thermophys.* **2010**, *31*(1), 199.
- [42] U. Polimeno, M. Meo, D. P. Almond, S. L. Angioni, *Appl. Compos. Mater.* **2010**, *17*(5), 481.
- [43] I. Y. Solodov, J. Wackerl, K. Pfeleiderer, G. Busse, *Appl. Phys. Lett.* **2004**, *84*(26), 5386.
- [44] F. Semperlotti, S. C. Conlon, *J. Acoust. Soc. Am.* **2010**, *127*(2), EL48.
- [45] A. Lamberti, F. Semperlotti, *Smart Mater. Struct.* **2013**, *22*(12), 125006.
- [46] I. Y. Solodov, *J. Nondestruct. Eval.* **2014**, *33*(2), 252.
- [47] I. Y. Solodov, J. Bai, S. Bekgulyan, G. Busse, *Appl. Phys. Lett.* **2011**, *99*(21), 211911.
- [48] K. L. Reifsnider, E. G. Henneke, W. W. Stinchcomb, The mechanics of vibrothermography, in *Mechanics of Nondestructive Testing*, (Ed: W. W. Stinchcomb), Plenum Press, New York **1980**, 249.
- [49] L. Pieczonka, M. Szewdo, Vibrothermography, in *Advanced Structural Damage Detection: From Theory to Engineering Applications*, (Eds: T. Stepinski, T. Uhl, W. J. Staszewski), Chichester, Wiley 233–261.
- [50] Monit SHM. Vibrothermography. Available at: <http://www.monitshm.pl/en/index.php?loc=vibrothermography>. **2016**.
- [51] Klepka A, Pieczonka L, Staszewski WJ, Aymerich F. Application of local defect resonance method to structural damage detection. Proceedings of the International Workshop on Structural Health Monitoring Stanford California. **2013**.

How to cite this article: Pieczonka L, Zietek L, Klepka A, Staszewski WJ, Aymerich F, Uhl T. Damage imaging in composites using nonlinear vibro-acoustic wave modulations. *Struct Control Health Monit.* 2017;e2063. <https://doi.org/10.1002/stc.2063>